Indian Journal of Chemical Technology
Vol. 26, November 2019, pp. 483-493

Statistical optimization of the Zinc chloride activated biomass using Box-Behnken design

Shilpi Das*,[1] & Susmita Mishra[2]

[1]ResearchScholar, Department of Chemical Engineering, N.I.T, Rourkela 769 008, Odisha, India.

[2]Professor, Department of Chemical Engineering, , N.I.T, Rourkela 769 008, Odisha, India.

E-mail: shilpiavenue@gmail.com

Received 18 April 2018; accepted 8 August 2019

The preparation of activated carbon from an economically sustainable precursor *Limonia acidissima* shell (an agricultural waste) by chemical activation method has been explored in the present study. This investigation emphasizes the application of a statistical tool, Response surface methodology (RSM) coupled with Box-Behnken design (BBD) to optimize the experimental conditions for the preparation of activated carbon from lignocellulosic wastes activated with $ZnCl_2$. The chemical activation is conducted at a different combination of impregnation ratios (IR), activation time and carbonization temperatures as suggested by the Design Expert software. The influences of these parameters on the responses i.e. iodine no. and yield of activated carbon has been investigated. Simultaneous optimization is performed using desirability approach. The desirability value reported for AC-$ZnCl_2$ is 0.653. The carbon yield and iodine adsorption value approached 49.67% and 928.58 mg/g under the optimal conditions of impregnation ratio (1), activation time(57.09 min),and carbonization temperature (436.52°C). Important physicochemical properties of the optimized activated carbon is further confirmed by FTIR analysis, TEM analysis etc.

Keywords: Activated carbon, Lignocellulosic biomass, Optimization

In recent years, the disposal of agroforestry waste has become one of the major global environmental problems. These by-products are produced as a result of the annual harvesting and processing of various agricultural crops grown around the world. They accumulate in various places resulting in water pollution, eutrophication, and high level of BOD as well as COD. Therefore, the sustainable conversion of these unsaleable wastes into useful products is becoming increasingly important[1]. Agricultural wastes are of lignocellulosic origin that comprises of cellulose, hemicellulose, and lignin along with the variety of functional groups that makes it a potential precursor for the production of activated carbon. There has been a plethora of research on the efforts to obtain low cost activated carbon from various agricultural wastes such as coconut shell[2], rice husk[3], sugarcane bagasse[4], hazelnut shell[1], jackfruit peel[5], corn cob[6], pistachio-nut[7]etc. Thus, the search for eco-friendly ways of the disposal of agricultural wastes has triggered research emphasizing on the utilization of by-products as a precursor for the production of activated carbon.

Activated carbon, an amorphous solid is the resultant product of the activation of various types of carbonaceous materials such as wood, peat, coal etc. It is known for its versatile applications of industrial significance such as treatment of waste water containing heavy metals and other inorganic pollutants by adsorption, manufacture of electrodes and capacitors, etc.[8,9]. The surface areas generally vary within the range 500-1400 m^2/g, however in some cases, the carbons are found to have a surface area >2500 m^2/g[10,11]. Basically, the activated carbon can be prepared by two different procedures: physical activation and chemical activation. The physical activation results in the development of a large internal surface area and creation of pore structure but due to excessive burn-off of the external carbon surface, there is a decrease in average particle size which leads to a reduction in the yield of the final product. In chemical activation, the precursor is impregnated with any one of the activating agents such as H_3PO_4, $ZnCl_2$, H_2SO_4, KOH etc. and heat treated under an inert atmosphere at a relatively low temperature (400-800°C)[12,13]. These activating agents act as dehydrating agents which promote the formation of cross-links leading to the development of a rigid matrix, resulting in an increase in the carbon yield. Chemical activation using $ZnCl_2$ has been

studied by several researchers at different experimental conditions and has been applied to different lignocellulosic materials.

Thus in the present study, an economically sustainable material *Limonia acidissima* shell has been chosen as the precursor for the preparation of activated carbon. It is a strong-shelled tropical fruit which belongs to Rutaceae family and is grown throughout India, Bangladesh, and Srilanka. It may be known as wood apple, elephant apple and locally known as Kathbel, Kaitha, Kapitha etc. The appearance of the fruit is similar to Bael (*Aegle Marmelos*) fruit. The fruit shell is a biowaste and has the potential to be converted into useful value-added adsorbent. No studies have been reported yet regarding the preparation of activated carbon from this feedstock.

To optimize the process conditions for the production of effective activated carbon at minimum time,the use of the statistical model is generally employed[14]. RSM is one of the powerful approaches to test the several parameters employing a minimum number of experimental trails[15]. Generally, it consists of a collection of mathematical and statistical procedure which builds an experimental design that can analyze the effect of parameters on the response variable to figure out the optimized response[16]. BBD, one of the RSM methods was employed for the optimization of process variables because it is very useful and efficient. It can determine the factors of the quadratic model, detect lack of fit of the model, and looks more desirable if the points are at the midpoint of edges of the process and at the center[17-19]. Therefore, in the present investigation, the main objective would be to optimize the preparation of activated carbon from *Limonia acidissima* shell to assess the effect of the process conditions such as carbonization temperature (A), impregnation ratio (B) of the activating agent i.e.$ZnCl_2$ and activation time (C). A series of experiments were carried out with values of A,B, and C included in the suitable range. Moreover, the process performance of activated carbon is investigated by total yield and iodine adsorption value.

Experimental Section

Materials

Limoniaacidissima shell was used as a precursor in the present study for the preparation of activated carbon via chemical activation. Prior to use, the shells were washed repeatedly with water to remove the surface-adhered particles followed by sun-drying to reduce the moisture content. Subsequently, the dried shells were crushed and subjected to grinding and screening technique to reduce their particle size to 1.0-1.5 mm. And, finally stored in airtight packets for further experimentation. All the chemicals used in this present work were of analytical grade.

The proximate and ultimate analysis of the raw sample is presented in Table 1.

Activated Carbon Production

Chemical activation of *Limonia acidissima* shell

The granular particles of the precursor material was impregnated with $ZnCl_2$ solution. Since $ZnCl_2$ is in solid form, the weight ratio was calculated based on the following Eq.

$$\text{Impregnation ratio (IR)} = \frac{\text{Wt of activating agent (g)}}{\text{Wt of powdered precusor (g)}} \quad \ldots (1)$$

About 2.5-5 g of $ZnCl_2$ has been dissolved in distilled water followed by the addition of 5 g of dried precursor to the $ZnCl_2$ solution. The mixing was performed at 90°C for 4 h to ensure the access of activating agents to the interior of the precursor, and then subjecting the mixture to increase in temperature until complete dryness.

Carbonization of Impregnated shell

After the completion of the impregnation process, the samples had been placed in a ceramic crucible and inserted at the middle of the horizontal electric tubular furnace (Bysakh & Co.) with tube dimensions of 104 mm length and 70 mm diameter in an inert atmosphere, with a constant N_2 flow of 100 mL/min. The resulting chemical loaded samples were pyrolyzed in the furnace from room temperature to a preselected final temperature in the range of (400-700°C) with a constant heating rateof 5°C/min for a different length of carbonization time i.e. (10-60 min). After the completion of the carbonization process,

Table 1 — Proximate and elemental analysis of *Limonia Acidissima* shell

Proximate analysis	Ultimate analysis
Moisture content (%) - 11.8%	Carbon (%) - 70.17%
Volatile matter (%) - 68.414 %	Hydrogen (%) - 3.771%
Ash content (%) - 5.09%	Nitrogen (%) - 1.6%
Fixed carbon (%) - 14.696%	Sulphur (%) - 0.174%
	Oxygen (%) - 24.285%

the content was cooled down and ground to powdered form in the mortar and pestle. It was washed subsequently with acid and followed by distilled waterto remove the excess activating agents from the surface of activated carbon until the *p*H of the washing effluent remains constant. The samples were finally dried at 105°C overnight to eliminate the adsorbed water and stored in sealed bags for further analysis.

Experimental design methodology

Response surface methodology (RSM) is a statistical method employed for obtaining optimal conditions for maximum yield as well as iodine adsorption value. It was used to correlate the relationship among the effects of process variables on the preparation of activated carbon. The experimental design was constructed through Design Expertsoftware version 7 (Stat-Ease, Minneapolis, U.S.A) using Box-Behnken design (BBD) to experimental data. BBD was concluded as the most efficient design method as compared to the various response surface designs i.e. (BBD, CCD, Dohelert matrix and three level factorial design). Impregnation ratio, activation time (min), and carbonization temperature (°C) were chosen as independent variables and each of them was examined in 3 levels (-1,0,+1), -1 denoted low level, +1 for high level and 0 for the midpoints to evaluate the experimental error. The various levels and range of factors used in this study for the preparation of optimized activated carbon i.e AC-($ZnCl_2$) are shown in Table 2.

The total no. of runs (N) computed were 17 which included 12 factorial points with 5 center points as mentioned in Eq. below:-

$$N=2k\,(k-1)+C_o=2\times3(3-1)+5=17 \quad \ldots (2)$$

Also, the relationship between the predicted response and the process parameters was expressed by the following second-order polynomial regression model equation:-

Table 2 — Level of parameters in Box-Behnken experimental design

Parameters	Factors	AC- $ZnCl_2$	
		(-1)	(+1)
Impregnation ratio	A	0.5	1
Activation time (min)	B	10	60
Activation temperature (°C)	C	400	700

$$Y=\beta_0+\sum_{i=1}^{k}\beta_i X_i+\sum_{i=1}^{k}\beta_{ii}X_i^2+\sum_{i=1}^{k-1}\sum_{j=2}^{k}\beta_{ij}X_iX_j \quad \ldots (3)$$

Where $\beta_0, \beta_i, \beta_{ii}, \beta_{ij}$ are the regression coefficients and Y is the predicted response. β_0 is the constant term, β_i is the linear effect term, β_{ii} is the quadratic effect term, and β_{ij} is the interaction effect term. The results and the coefficients of the quadratic equation were analyzed using the analysis of variance (ANOVA) by Design Expert software.

Optimization analysis

The popular approach for assessing the simultaneous optimization of the multiple responses having various input variables is Desirability function. It involves the conversion of each predicted response (Y_i) into an individual desirability function, (d_i) on the basis of researcher's priorities and desires while building the optimization procedure. The desirability function varies over the range

($0 \leq d_i \leq 1$) with $d_i=0$ indicating the undesirable value of Y_i and di = 1, if the response achieves the target value.

Characterization of the raw sample and the optimized activated carbon

Thermogravimetric analysis (TGA) represents an important analytical technique used to determine the pyrolysis behavior of the raw sample. The TGA-DTA curves describe the degradation process as well as thermal stability occurring at different temperatures. TGA of the lignocellulosic material has been carried out by using the DTG-60H instrument. Around 20-30 mg of the sample was taken in a silica crucible and heated over the temperature range of (0-900°C) at a heating rate of 5°C/min under a constant N_2 flow rate of 25 mL/min.

N_2 adsorption-desorption experiments were conducted at -196°C to assess the specific surface area as well as the pore structure characteristic of the optimized activated carbon using a surface area analyzer (Quantachrome, U.S.A). Prior to the experiment, the samples were degassed at a higher temperature for 5-6 h. to remove all the physisorbed species from the surface of the adsorbent. The isotherms were measured over a relative pressure range (p/p_o) approximately from 0.025 to 1.

The point of zero charge (pH_{ZPC}) is the *p*H of the solution at which the net charge on the surface of the

activated carbon is zero. In the field of environmental science, pH_{ZPC} denotes the adsorption of harmful ions by asubstrate. It was determined using the salt addition method commonly known as "drift method". The procedure is described as follows: Activated carbon (0.2 g) was mixed with about 40 mL of 0.1 M $NaNO_3$ solution in different flasks. The initial *p*H value (pH_i) of the solution was adjusted to 2-11 by the addition of either 0.1M HNO_3 or 0.1M NaOH. The flasks were sealed immediately with parafilm and agitated in the shaker at 110 rpm for 24 h before the final *p*H value (pH_f) of the filtrate was recorded. The (ΔpH) (i.e. the difference between the initial and final *p*H) was plotted against the initial pH value (pH_i). The point of intersection (i.e. the point at which $\Delta pH=0$) is considered as zero point charge[20].

FTIR Analysis was performed on a Perkin-Elmer, Spectrum Two using the KBr pellet technique. The spectra were recorded from 4000 to 400 $cm^{-1}$by 8 scans per sample with 4 cm^{-1} resolution. The functional groups on the surface of the raw sample and optimized activated carbon was detected through this analysis.

The microscopic studies for the image analysis of the raw precursor and the optimized activated carbon were carried out on a FET Tecnai TF $30G^2$ Transmission electron microscope SUPER TWIN with STEM and EDS (Bruker, Germany) operated at an accelerating voltage of 300 kV. Bright Field images and selected-area ring diffraction (SAED) patterns were acquired using this microscope. The compositional verification and elemental mapping was done by TEM equipped with EDS mapping in the TEM (STEM) mode. The surface topography of the raw feedstock and optimal activated carbon was investigated by the Field Emission Scanning Electron Microscope (FESEM-NOVA NANO SEM450). A thin layer of platinum was coated on the samples for charge dissipation during FESEM imaging. The coater was operated using a current of 30 mA for 3 min. The coated samples were then transferred to the FESEM specimen chamber and the surface texture was observed. X-ray diffraction patterns (XRD) were recorded using Rigaku Ultima IV. The instrument was equipped with Cu Kα radiation (40 kV, 40 mA) with the wavelength of ($\lambda = 1.78901$ Å) at a step size of 0.02. The samples were initially placed in the XRD sample port. The scan rate was 3^o/min and the patterns were recorded for 2θ values of 5-80^o. The obtained data was analyzed by X'Pert High Score software.

Results and Discussion

Thermal Characterization

The structural evolution and the thermal stability of the lignocellulosic biomass was analyzed by TGA test. The TGA thermogram of *Limonia Acidissima*, shell as shown in the Fig. 1. The thermal degradation of the sample showed the three weight loss regions. The curves showed that the active pyrolytic zone was in between the temperature range of 200-500°C[21]. In this case, the first stage occurring at temperature range approximately from 26-150°C represented the evaporation of moisture content, second decomposition marked the beginning of the de-volatilization process i.e. the formation of volatiles mainly CO and CO_2 indicating a wt. loss of 48.18%. And, the third step was characterized by slight rise in mass loss rate (20.04%) of residue char of shell at 360-450°C. Above this the wt. loss became almost constant till the end of the decomposition[22, 23].

The DTG curves as shown in Fig. 1 represented the wt. loss rate (dm/dt) of the raw *Limonia Acidissima* shell. It was used to determine the amount of lignin, cellulose and hemicellulose content in the biomass. It highlights the zone of reaction where the various reaction steps are occurring over the entire temperature range. The spectrum presented three main peaks among which the 1st endothermic peak at around 78°C belonged to the removal of moisture content. Hemicellulose is thermally less stable compared to cellulose and lignin due to its amorphous structure and so it started decomposing easily with the mass loss in the temperature range of 204-253°C. The next phase between 264-374°C with a peak at 286°C was attributed to cellulose decomposition which required higher energy due to the presence of strong hydrogen bonding. And, finally the presence of a peak at 463°C corresponded to traces of lignin in the

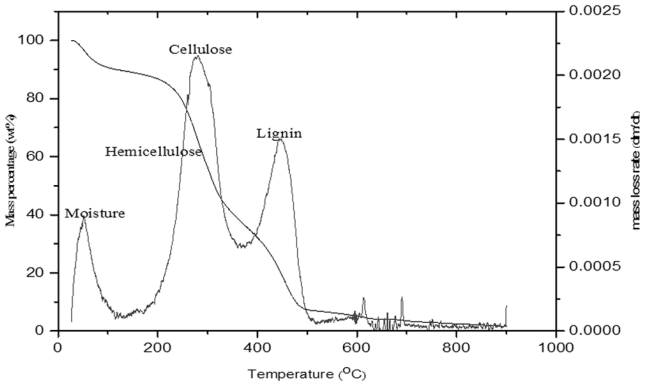

Fig. 1 — TGA and DTG curve of raw *Limonia Acidissima* shell

sample. Lignin beingthe most complex structure is assumed to decompose slowly over a broad temperature range from ambient to 900°C developing the flat trailing section of the DTG curve resulting in a high char yield. Literature study revealed that the thermal analysis resulted in the pyrolysis of hemicellulose mainly at 200-315°C and that of cellulose at 250-400°C and since lignin is difficult to be decomposed as its weight loss happened in a wide range of temperature from 150-900°C[24].

Optimization of preparation conditions via RSM

In the present study, the 3-factor 2-level Box-Behnken experimental design has been utilized to investigate the correlation between the combined effects of individual parameters to both the responses. The experimental results of the combination of all the factors and their corresponding predicted responses for each run of AC-$ZnCl_2$are tabulated in Table 3.

Factors AC-$ZnCl_2$

Based on these results, the polynomial equations obtained in coded units showing the empirical relationship between the responses and independent variables are given below:-

AC-$ZnCl_2$

Yield = +44.72 + 0.65*A -0.64*B - 5.33*C + 0.24*A*B + 0.13*A*C + 0.83*B*C + $0.23*A^2$- $0.47B^2 + 2.65C^2$ … (4)

Iodine value = +1148.64 + 62.19*A + 70.19*B + 297.19*C + 40.17*A*B + 6.54*A*C -109.59*B*C - $47.35*A^2 – 20.74*B^2$-$280.00*C^2$ … (5)

Statistical evaluation

A statistical analysis of variance (ANOVA) based on BBD was performed with Design-Expert software, version 7.0(Stat-Ease, Minneapolis, U.S.A) to check the fitness and significance of the model co-efficient. Tables 4, 5 summaries the ANOVA results for both the responses of the optimized AC-$ZnCl_2$.

Table 4 — ANOVA results of the quadratic model for the yield of AC-$ZnCl_2$

Source	Sum of squares	df	Mean square	F-value	p value (Prob>F)
Model	267.09	9	29.68	52.48	<0.0001
A-IR	3.38	1	3.38	5.98	0.0444
B-Time	3.28	1	3.28	5.79	0.0470
C-Temp	226.85	1	226.85	401.16	<0.0001
AB	0.24	1	0.24	0.42	0.5355
AC	0.063	1	0.063	0.11	0.7493
BC	2.72	1	2.72	4.81	0.0643
A^2	0.22	1	0.22	0.40	0.5493
B^2	0.93	1	0.93	1.64	0.2410
C^2	29.58	1	29.58	52.31	0.0002
Residual	3.96	7	0.57		
Lack of fit	3.48	3	1.16	9.64	0.0266

R^2 = 0.9854, Adj.R^2 = 0.9666, Pred.R^2 = 0.7920, Adequate Precision = 21.327, CV% = 1.64, Standard Deviation = 0.75

Table 3 — Box-Behnken matrix for the experimental & predicted values of Yield and Iodine Adsorption value of AC-$ZnCl_2$

Runs	A	B(min)	C (°C)	Yield (%)		Iodine no (mg/g)	
				Actual	Predicted	Actual	Predicted
1	0.75	35	550	44.14	44.72	991.60	988.34
2	0.5	35	400	44.82	45.53	1088.57	1032.38
3	1.00	10	550	43.66	42.95	992.19	1048.38
4	0.75	35	550	45.32	44.74	1249.84	1253.10
5	0.75	35	550	52.46	52.40	523.71	468.45
6	0.50	35	700	53.64	53.46	582.08	579.75
7	0.75	35	550	41.32	41.50	1047.72	1049.75
8	0.75	60	700	43.00	43.06	1131.96	1187.22
9	0.50	60	550	54.22	53.69	312.41	370.93
10	0.75	60	400	50.00	50.77	731.41	730.48
11	1.00	60	550	42.16	41.39	1183.56	1184.49
12	1.00	35	400	41.24	41.77	1164.20	1105.68
13	0.75	10	700	44.74	44.72	1104.35	1148.64
14	0.75	35	550	44.24	44.72	1075.13	1148.64
15	0.75	10	400	44.72	44.72	1128.89	1148.64
16	0.5	10	550	45.22	44.72	1230.31	1148.64
17	1.00	35	700	44.70	44.72	1204.53	1148.64

Table 5 — ANOVA results of the quadratic model for the iodine no. of AC-$ZnCl_2$

Source	Sum of squares	df	Mean square	F-value	p value (Prob>F)
Model	1.184E+006	9	1.316E+005	25.00	0.0002
A-IR	30941.89	1	30941.89	5.88	0.0458
B-Time	39410.28	1	39410.28	7.49	0.0291
C-Temp	7.066E+005	1	7.066E+005	134.21	< 0.0001
AB	6454.52	1	6454.52	1.23	0.3048
AC	171.23	1	171.23	0.033	0.8620
BC	48039.87	1	48039.87	9.13	0.0194
A^2	9438.95	1	9438.95	1.79	0.2224
B^2	1812.00	1	1812.00	0.34	0.5758
C^2	3.301E+005	1	3.301E+005	62.70	< 0.0001
Residual	36851.88	7	5264.55		
Lack of fit	19302.81	3	6434.27	1.47	0.3501

R^2=0.9698, Adj.R^2=0.9310, Pred.R^2 = 0.7247, Adequate Precision = 15.852, CV% = 7.37, Standard Deviation = 72.56

R^2 = 0.9854, Adj.R^2 = 0.9666, Pred.R^2 = 0.7920, Adequate Precision = 21.327, CV% = 1.64, Standard Deviation = 0.75

According to ANOVA, the larger value of F and a smaller value of p i.e. ($p < 0.05$) indicates that the model is statistically significant. Therefore, among the reported values mentioned, the (Prob>F) value was found to be less than 0.0001 for the yield % of AC-$ZnCl_2$, with F value of 52.48 indicated a significant model fit. The Fisher F test with a very low probability value of 0.0002 also demonstrated a high significance of the model of iodine value. The higher value of the coefficient of determination (R^2) i.e. 0.9854 and 0.9698 for the responses of AC-$ZnCl_2$ indicated a good correlation between the measured and predicted responses.

The "Pred R-squared" was found to be in reasonable agreement with the "Adj R-squared" value for the yield% of the activated carbon since their difference was less than 0.2 whereas regarding iodine value the difference between adj R-squared and pred R-squared was more than 0.2 indicating a blocking effect for which model reduction was necessary. "Adeq Precision" measures the signal to noise ratio and a ratio > 4 is desirable. Since for the present study, the signal to noise ratio was found to be > 4 in all the cases, so the quadratic model could be used to navigate the design space. Simultaneously, a low value of the co-efficient of variation (CV) denoted good accuracy and reliability of experiments[25].

In this study, the independent parameters including IR (A), activation time (B), carbonization temperature (C), the interaction effect of time and temperature (BC) and the second-order effect of temperature (C^2) of the response iodine no. of AC-$ZnCl_2$ are significant parameters with p-value< 0.05 whereas the other terms as shown in Table 4 are insignificant with p-value> 0.1. The model terms A, B,C, C^2 were also observed as significant for the response yield%, however, the rest of the terms did not show any significant impact. Thus, it's observed that the values of Prob>F less than 0.05 are significant terms whereas the model terms with p-value>0.05 are considered statistically insignificant[26].

Response surface and contour plots

The 3-D plots are a function of two factors maintaining all other parameters at fixed levels are helpful in understanding the interaction effect of the two factors. The 3-D response surface and their corresponding contour plots for the optimized AC-$ZnCl_2$ are the graphical representation of the refined quadratic equations obtained after model reduction, which demonstrate the relationship between the effect of experimental variables, and the responses are shown in Fig. 2 and Fig. 3.

Iodine adsorption

From the Fig. 2, the response surfaces showed changes in Y_2 (iodine adsorption value) with the variation in activation time and carbonization temperature. The iodine value increases when the temperature is increased from 400-700°C because increased temperature enhances the dehydration of the activating agent and increases the release of volatile matter resulting in the development of the porous structure. However, at a higher temperature, it decreases due to heat shrinkage of the carbon

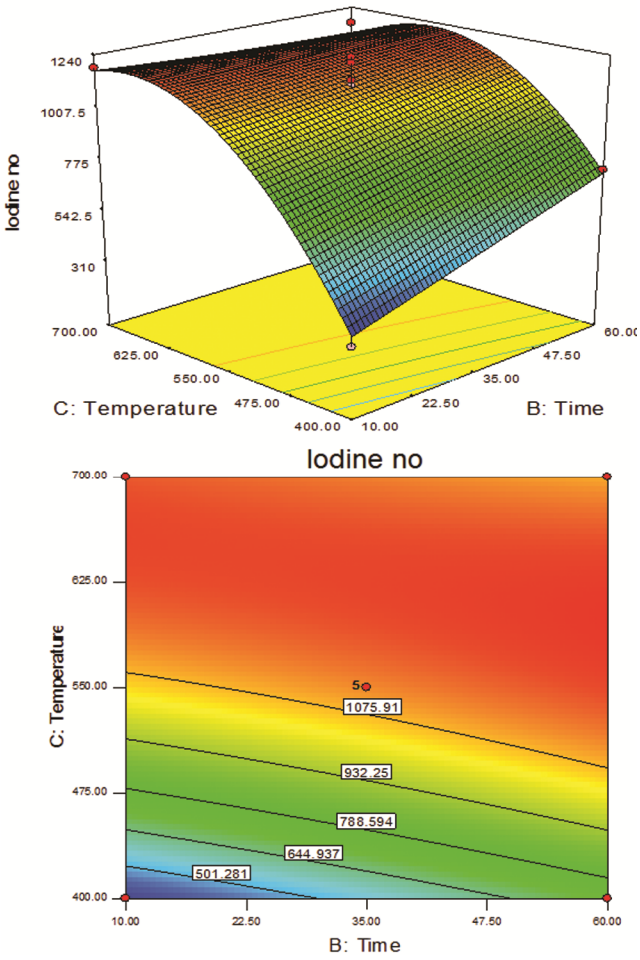

Fig. 2 — Response surface plot and the contour plots showing the impact of activation time and carbonization temperature on the iodine value of AC-$ZnCl_2$

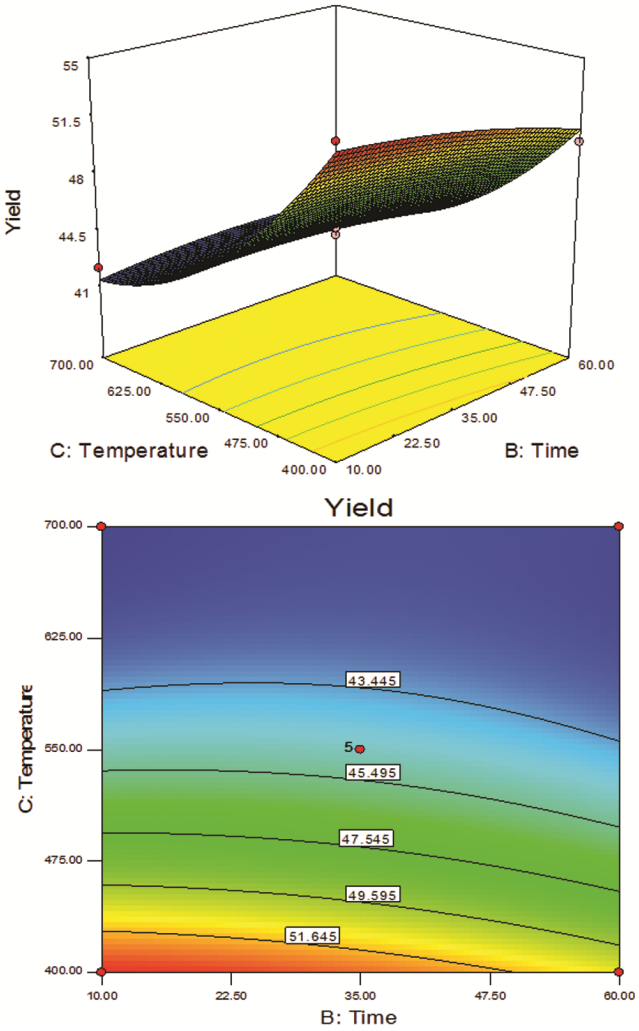

Fig. 3 — Response surface plot and the contour plots showing the impact of carbonization temperature and activation time on the yield% of AC-$ZnCl_2$

structure resulting in a decrease in the surface area[27]. The carbonization time was studied in the range of 10-60 min. The contour plots showed the straight lines parallel to activation time axis revealed that time had little effect on the iodine adsorption value of AC-$ZnCl_2$ i.e. the response did not significantly change with increasing time.

Yield

The yield can be defined as the wt. of activated carbon produced to the mass of raw material used. Figure 3 represents the response surface plot for the yield of AC-$ZnCl_2$ as a function of carbonization temperature and activation time. The weight loss of the activated carbon increased with the increasing temperature due to the loss of volatiles, promotion of carbon burning-off upon heating and the quantity of volatiles evolved increased due to an increase of temperature. The results indicated that the higher value of yield was obtained at lower temperature whereas activation time had almost a negligible effect on the yield of the carbon saving energy consumption.

Process optimization

It is essential to optimize the process parameters for the mass production of activated carbon using less amount of raw materials. Activated carbon with high yield and good adsorption capacity are desired because it will increase the competitiveness of activated carbon in the marketplace. Therefore, by applying the RSM method, optimization of the process parameters has been carried out for maximum yield and high iodine adsorption value. But, it is still difficult to optimize the two responses under the same process variables because the interest regions are

different. In order to compromise between the two responses, Design-Expert software used a factor named "desirability function" to show the best suitable condition for the optimized carbon. The process parameters (Impregnation ratio, activation time, carbonization temperature) in the present analysis were selected "within the range" and the responses wee set as "maximum" by Numerical optimization of the desirability function. The predicted parameters of AC-$ZnCl_2$ are IR-1, activation time- 57.09 min and carbonization temperature-436.52°C resulting in 49.67% yield and iodine no. of 928.58 mg/g with an overall desirability value of0.653. The desirability ramp for Numerical optimization is shown in Fig. 4. For their validation, confirmatory experiments were conducted (Table 6) using the optimized parameters and the results obtained were very closely related with the data obtained from Box-Behnken analysis.

Characterization

BET Analysis

N_2 adsorption-desorption isotherm

N_2 adsorption is one of the most convenient procedure to characterize the adsorbent. It illustrates the nature of adsorption-desorption process occurring on the surface. The isotherm is expressed as the volume of gas adsorbed as a function of relative pressure. Figure 5 shows the N_2 adsorption-desorption isotherm of the optimized AC-$ZnCl_2$ at 77.50K. According to Brunauer-Deming-Deming-Teller (BDDT) theory, the basis of modern IUPAC classification, the physisorption isotherms are grouped into six types. The curve of AC-$ZnCl_2$ reported the features of Type I as seen in Fig. 5 isotherm but the adsorption capacity continued to increase with an increase in relative pressure upto $p/p_o \cong 1$ giving rise to an apparent hysteresis loop during desorption. It has been already mentioned in the literature that difference between the curvature of desorption branch and adsorption can be assumed as the presence of hysteresis loop which usually closes at relative pressure $p/p_o \approx 0.42$. But, it's seen that the closure part of the loop has occurred at very low pressure. The desorption branch persists down to very low pressure region giving rise to the well-known low pressure hysteresis phenomenon (LPH)[28]. A deficient outgassing treatment or lack of equilibrium might have given rise to such type of hysteresis phenomenon. But, the sample had been initially degassed at 180°C for 5 h and due to poor results obtained, the process was repeated again at much higher temperature i.e. 300°C for 6 h. There was hardly any change noticeable in the shape of hysteresis. Thus, it is concluded that occurrence of LPH may be due to irreversible uptake which may be ascribed to the presence of pores of the same width of the adsorbate molecule or swelling of the non-rigid carbon walls considering desorption branch responsible for these causes. Due to these previously mentioned reasons, further BET analysis of AC-$ZnCl_2$was not executed.

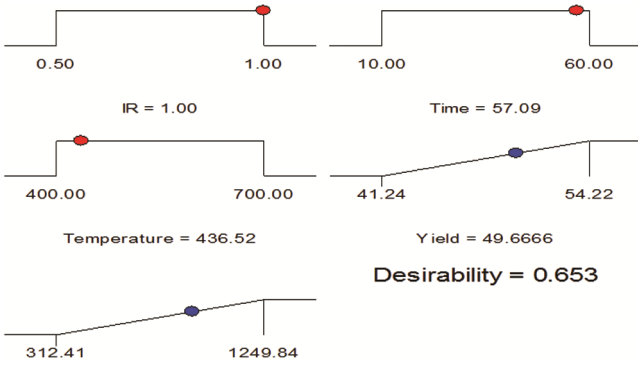

Fig. 4 — Desirability ramp for Numerical optimization of AC-$ZnCl_2$

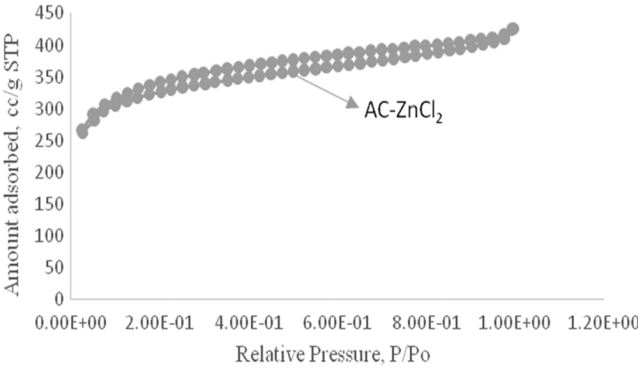

Fig. 5 — Nitrogen adsorption-desorption isotherm of AC-$ZnCl_2$

Table 6 — Model Validation

Impregnation ratio	Activation Temperature	Activation Time	Yield (%)		Iodine adsorption value (mg/g)	
			Predicted	Experimental	Predicted	Experimental
1	436.52°C	57.09 min	49.66664	7.65	928.5891	0.89

Surface chemistry determination

FTIR Analysis

The FTIR spectra of the raw sample and the optimized AC-$ZnCl_2$ were collected for the qualitative determination of their chemical structure. Figure 6 showed the FTIR spectrum of the raw feedstock in the range of 400-4000 cm^{-1}. The wide transmittance band at 3421.11 cm^{-1} represented the O-H stretch of the phenol and carbonyl groups. The peak at 2936.02 cm^{-1}, 1464.19 cm^{-1} is assigned to methylene group due to C-H stretching. The band at 2119.86 cm^{-1} is a characteristic of C-C stretching vibration of alkyne groups. A medium band at 1737.90 cm^{-1} was the C=O stretching, indicating the presence of an aldehyde or ketone in the feedstock. Two bands approximately at 1508 cm^{-1} and 1635.57 cm^{-1} denoted the presence of alkenyl (C=C) vibration in the aromatic rings. The

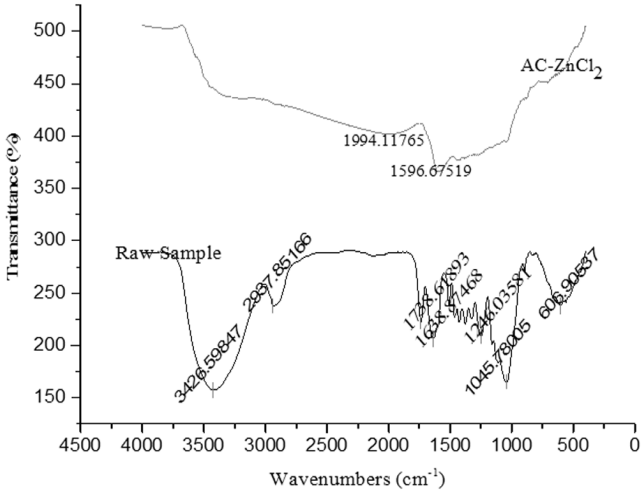

Fig. 6 — FTIR Spectrum of the raw*Limonia acidissima* shell and AC-$ZnCl_2$

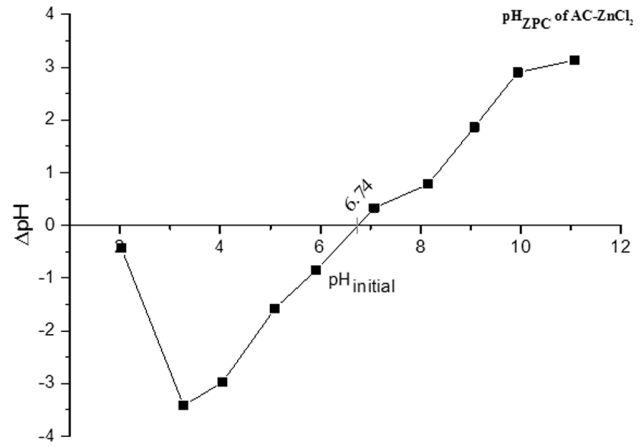

Fig. 7 — pH_{ZPC} determination using salt-addition method for optimized AC-$ZnCl_2$

1320-1000 cm^{-1} is associated with C-O stretching vibration in alcohols, carboxylic acid, esters, and ethers. The region below 1000 cm^{-1} is complex since it becomes difficult to assign all the absorption bands due to it's unique pattern often called as the fingerprint region. The signal in 897.45 cm^{-1} is associated with the β-glycosidic links between monosaccharides unit in biomass.

The FTIR spectrum of AC-$ZnCl_2$ displayed very less no. of absorbance bands compared to raw feedstock due to decomposition of cellulose, hemicellulose, and lignin in the *Limonia acidissima* shell during carbonization and activation process. It was observed that the absorbance bands had peaks at 1994.12 $cm^{-1}$and 1596.68 cm^{-1} respectively. The most significant absorbance peak was noticed at 1596.68 cm^{-1} indicating the presence of quinones and lactones[29-31]. Thus, the presence of characteristic bands gave a vivid explanation of the surface chemistry of the optimized activated carbon.Thus, $ZnCl_2$ on reaction with lignocellulosic biomass forms biomass-$ZnCl_2$ complex and liberates water molecules. The biomass-$ZnCl_2$ complex will be converted into char and volatiles followed by degradation of char into gases. During activation process, the role of $ZnCl_2$ is mainly in the catalytic dehydration. The swelling effects of zinc chloride are occurred by lateral bond breaking in the molecules leading to increased inter and intra voids. The interspaces between the carbon layers created by $ZnCl_2$ would develop the microporosity after $ZnCl_2$ was washed away by HCl and distilled water.

***p*H_{ZPC}**

The point of zero charge (*p*H_{ZPC}) was determined to investigate the electrical state of the synthesized adsorbent surface in solutions. It was observed that the optimized AC-$ZnCl_2$ showed the *p*H_{ZPC} value of 6.74 i.e. (*p*H_{ZPC}<7) at which the net charge of the adsorbent is zero. It exhibited the acidic property of less strength. The adsorbent surface is positively charged for *p*H<6.74 and it becomes negatively charged at *p*H value above 6.74. Therefore, for *p*H value<6.74 the adsorption will be unfavourable because of repulsive electrostatic interaction between metal ions and positively charged functional groups. The maximum adsorption will occur at *p*H above *p*H_{zpc} value when the adsorbent surface is negatively charged. Thus, it demonstrated the strong dependence nature of the *p*H_{ZPC} value of the carbon on the chemical activation method used.

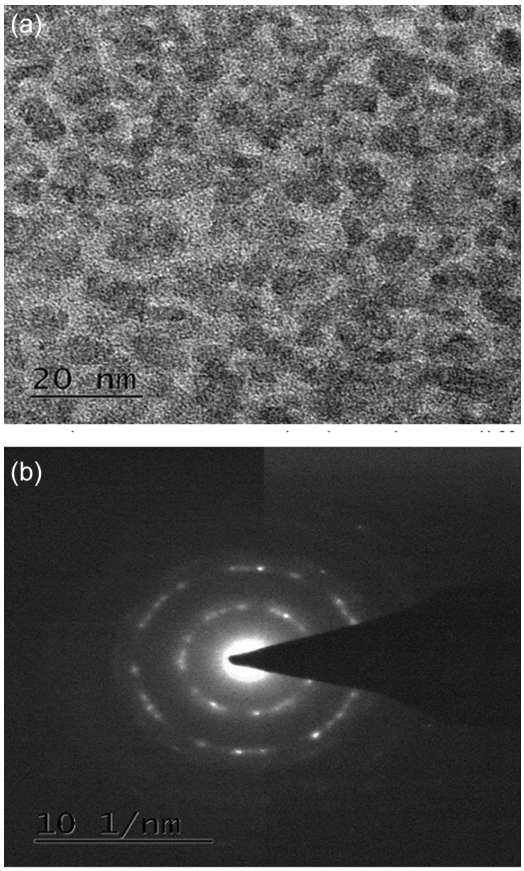

Fig. 8 — TEM and selected area diffraction pattern image of AC-$ZnCl_{2b}$

Morphology determination

TEM-EDX analysis

Image analysis has been applied to the TEM observation of activated carbon, in order to evaluate the pore structure visually. The bright field images revealed the development of microporous structure in carbon sample upon chemical activation of the precursor. Structural changes were observed in the samples as shown in Fig. 8a. The dark spots were considered to be the pores. The random arrangement of the small segments of hexagonal graphene layers resembled the turbostratic carbons. The slit-shaped pores had been assigned to the AC-$ZnCl_2$. TEM-Selected area electron diffraction (SAED) pattern as shown in Fig. 8b was performed to obtain the electron diffraction pattern of activated carbon which represented the pattern obtained from polycrystalline material. It consisted of small spots making up the concentric rings centered on a bright central spot representing the undiffracted electrons. The elemental mapping measurement of the activated carbon samples are shown in Fig. 9b which confirmed the co-existence and uniform dispersion of C-element mainly within the framework along with the location of other elements such as Ta, Zn,Oas later confirmed by EDX results (Fig. 9a). The elemental composition of AC-$ZnCl_2$ is (C- 69.83 %, Ta-22.67 %, Zn-5.23 %, O-1.72%, Cl-0.55 %). The Zn constituent is owing to

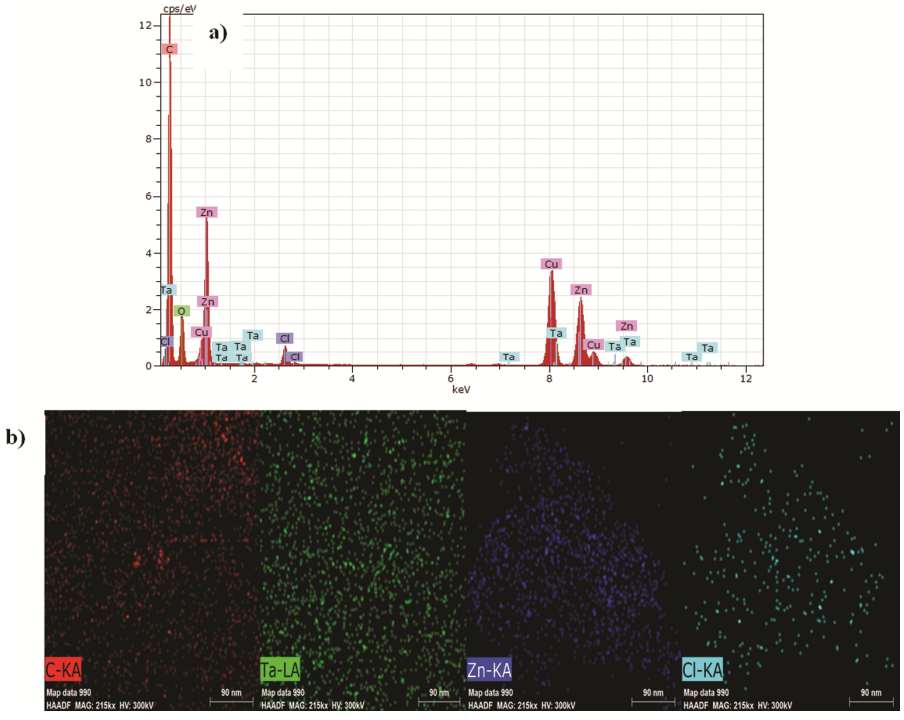

Fig. 9 — a) EDX spectrum and b) STEM mapping of AC-$ZnCl_2$

$ZnCl_2$ used for the chemical activation of the precursor and Cu came from the TEM grids being used.

Conclusion

The present investigation confirmed the feasibility of the preparation of quality AC-$ZnCl_2$ from lignocellulosic biomass i.e. *Limonia acidissima* shell, which would promote the ecological use of fuel, considered to be green energy, and eventually reduce the dependence of the world on the fossil fuel. The preparation of activated carbon has been conducted according to three factor, two-level Box-Behnken experimental design and the optimum conditions were attained by desirability approach in multi-response optimization. Various other sophisticated methods such as TEM, FTIR Analysis etc. has been successfully used to characterize the synthesized activated carbon. The investigated adsorbent is cost-effective as well as eco-friendly, which has the potential to be used for the adsorption of heavy metals being discharged from mining areas.

Acknowledgement

The authors are thankful to National Institute of Technology, Rourkela for providing the infrastructure and instrument facility for carrying out the research work.

References

1 Demirbas E , Dizge N, Sulak M T & Kobya M, *Chem Eng J*, 148 (2009) 480.
2 Aljeboree A M, Alshirifi A N & Alkaim A F, *Arab J* Chem, 10 (2017) S3381.
3 Mohanty K, Naidu J T, Meikap B C, Biswas M N & Bengal W, *Indian Eng Chem Res*, 45 (2006) 5165.
4 Karunarathne H D S S & Amarasinghe B M W P K, *Energy Procedia*, 34 (2013) 83.
5 Prahas D, Kartika Y, Indraswati N & Ismadji S, *Chem Eng Jl*, 140 (2008) 32.
6 Kumar A & Jena H M, *Appl Surf Sci*, 356 (2015) 753.
7 Baccar R, Bouzid J, Feki M & Montiel A, *J Hazard Mater*, 162(2009) 1522.
8 Sun Y & Webley P A, *Ind Eng Chem Res I*, 50 (2016) 9286.
9 Juan Y & Ke-qiang Q I U, *Environ Sci Technol*, 43 (2009) 3385.
10 Jiang Z, Liu Y, Sun X,Tian F, Sun F, Liang C, You W, Han C & Li C, *Langmuir*, 19 (2003) 731.
11 Karanfil T & Kilduff J E, *Environ Sci Technol*, 33 (1999) 3217.
12 Sekirifa M L, Hadj-Mahammed M, Pallier S, Baameur L, Richard D & Al-Dujaili A H, *J Anal Appl Pyrol*, 99 (2013) 155.
13 Ahmad A A, Hameed B H & Ahmad A L, *J Hazard Mater*, 170 (2009) 612.
14 Das S & Mishra S, *J Environ Chem Eng*, 5(2017) 588.
15 Vaez M, Zarringhalam Moghaddam A & Alijani S, *Indus Eng Chem* Res, 51 .(2012) 4199.
16 Varala S, Dharanija B, Satyavathi B, Basava Rao V V & Parthasarathy R, *Chem Eng J*, 302 (2016) 786.
17 Shakeel F, Haq N, Alanazi F K & Alsarra I A, *Ind Eng Chem* Res, 53 (2014) 1179.
18 Qiu P, Cui M, Kang K, Park B, Son Y, Khim E, Jang M & Khim J, *Central Europ J Chem*, 12 (2014) 164.
19 Rouquerol J, Llewellyn P & Rouquerol F, *Studies in Surface Science and Catalysis*, 160 (2007) 49.
20 Tran H N, Chao H P & You S J, *Adsorpt Sci Technol*, 36 (2018) 95.
21 Skreiberg A, Skreiberg O, Sandquist J & Sørum L, *Fuel*, 90 (2011) 2182.
22 Yang H, Yan R, Chen H, Lee D H & Zheng C, *Fuel*, *86* (2007) 1781.
23 Pasangulapati V, Ramachandriya K D, KumarA, Wilkins M R, Jones C L & Huhnke R L, *BioresourTechnol*, 114 (2012) 663.
24 Carrier M, Loppinet-Serani A, Denux D, Lasnier J M, Ham Pichavant F, Cansell F & Aymonier C, *Biomass Bioenerg*, 35 (2011) 298.
25 Zhang W, Zhu Z, Jaffrin M Y & Ding L, *Ind Eng Chem Res*, *53* (2014) 7176.
26 Zhu H, Fu Y, Jiang R, Yao J, Xiao L & Zeng G, *Ind Eng Chem Res*, *53* (2014) 4059.
27 Yang J & Qiu K, *Ind Eng Chem Res*, 50 (2011) 4057.
28 Silvestre Albero A M, Juárez-Galán J M, Silvestre Albero J & Rodríguez-Reinoso F, *J Phys Chem*, *C*116 (2012) 16652.
29 Tsai W T, Chang C Y, Lin M C, Chien S F, Sun H F & Hsieh M F, *Chemosphere*, 45 (2001) 51.
30 Sharma Y C & Uma Gode F , *J Chem Eng Data*, 55 (2010) 3991.
31 Song X, ZhangY & Chang C, *Ind Eng Chem Res*, 51 (2012) 15075.